

Transfinite Barycentric Coordinates for Arbitrary Planar Domains

Qingjun Chang, Kai Hormann

Faculty of Informatics, Università della Svizzera italiana, Switzerland

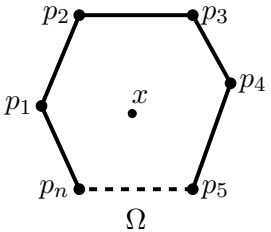
May 29, 2025 in St. Louis, USA

Generalized barycentric coordinates

Given a polygon Ω with n vertices p_1, p_2, \dots, p_n , and any $x \in \Omega$, find coordinates $\lambda(x) = [\lambda_1, \lambda_2, \dots, \lambda_n]$ such that

$$x = \sum_{i=1}^n \lambda_i(x)p_i, \quad \sum_{i=1}^n \lambda_i(x) = 1, \quad \lambda_i(v_j) = \delta_{i,j} = \begin{cases} 1, & i=j \\ 0, & i \neq j \end{cases}$$

- ❖ λ are *generalized barycentric coordinates* of x w.r.t. Ω .



Generalized barycentric coordinates

Given a polygon Ω with n vertices p_1, p_2, \dots, p_n , and any $x \in \Omega$, find coordinates $\lambda(x) = [\lambda_1, \lambda_2, \dots, \lambda_n]$ such that

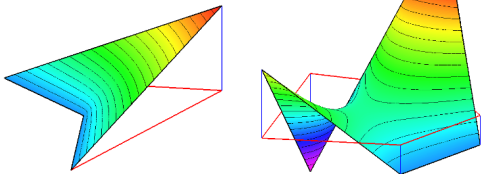
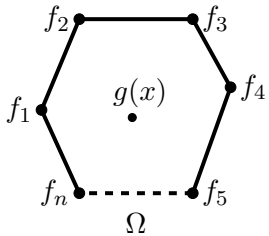
$$x = \sum_{i=1}^n \lambda_i(x)p_i, \quad \sum_{i=1}^n \lambda_i(x) = 1, \quad \lambda_i(v_j) = \begin{cases} 1, & i=j \\ 0, & i \neq j \end{cases}$$

- ❖ λ are *generalized barycentric coordinates* of x w.r.t. Ω .

Considering data f_1, f_2, \dots, f_n corresponding to the vertices, we can interpolate the data at any point $x \in \Omega$ by

$$g(x) = \sum_{i=1}^n \lambda_i(x)f_i, \quad \sum_{i=1}^n \lambda_i(x) = 1$$

(Generalized barycentric interpolation)



Generalized barycentric coordinates

Given a polygon Ω with n vertices p_1, p_2, \dots, p_n , and any $x \in \Omega$, find coordinates $\lambda(x) = [\lambda_1, \lambda_2, \dots, \lambda_n]$ such that

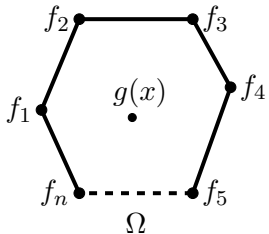
$$x = \sum_{i=1}^n \lambda_i(x)p_i, \quad \sum_{i=1}^n \lambda_i(x) = 1, \quad \lambda_i(v_j) = \delta_{i,j} = \begin{cases} 1, & i=j \\ 0, & i \neq j \end{cases}$$

- ❖ λ are *generalized barycentric coordinates* of x w.r.t. Ω .

Considering data f_1, f_2, \dots, f_n corresponding to the vertices, we can interpolate the data at any point $x \in \Omega$ by

$$g(x) = \sum_{i=1}^n \lambda_i(x)f_i, \quad \sum_{i=1}^n \lambda_i(x) = 1$$

(Generalized barycentric interpolation)



- ❖ When $n > 3$, such λ are usually **not unique**.
- ❖ Looking forward to finding λ that satisfy some properties.

Applications



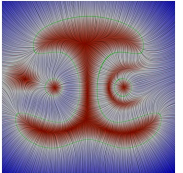
image warping



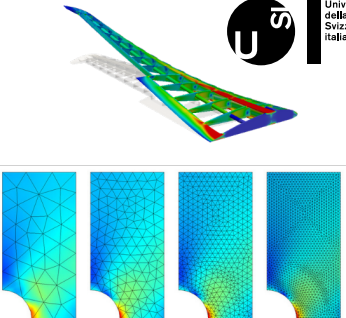
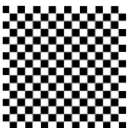
mesh deformation



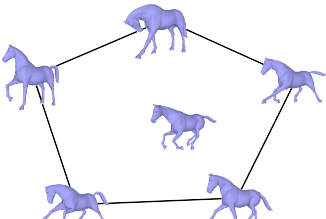
mesh parameterization



vector field interpolation

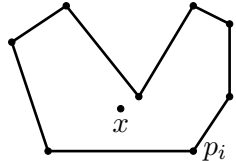


finite element method



mesh animation

Transfinite barycentric coordinates



Polygon: $\{p_i : i = 1, \dots, n\}$

generalized barycentric coordinates $\lambda_i(x)$

$$\sum_{i=1}^n \lambda_i(x) p_i = x$$

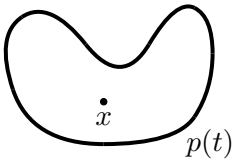
linear reproduction

$$\sum_{i=1}^n \lambda_i(x) = 1$$

partition of unity

$$\lambda_i(p_j) = \delta_{i,j}$$

Lagrange property



Curve: $\{p(t) : t \in [a, b]\}, p(a) = p(b)$

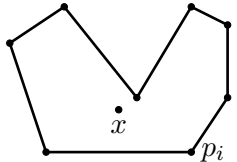
transfinite barycentric kernel $\lambda(x, t)$

$$\int_a^b \lambda(x, t) p(t) dt = x$$

$$\int_a^b \lambda(x, t) dt = 1$$

$$\lambda(p(s), t) = \delta(s - t)$$

Transfinite barycentric coordinates

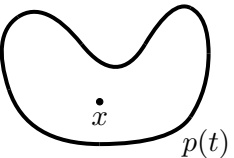


Polygon: $\{p_i : i = 1, \dots, n\}$

generalized barycentric coordinates $\lambda_i(x)$

$$\sum_{i=1}^n \mu_i(x)(p_i - x) = 0$$

$$\lambda_i(x) = \mu_i(x) \Bigg/ \sum_{j=1}^n \mu_j(x)$$



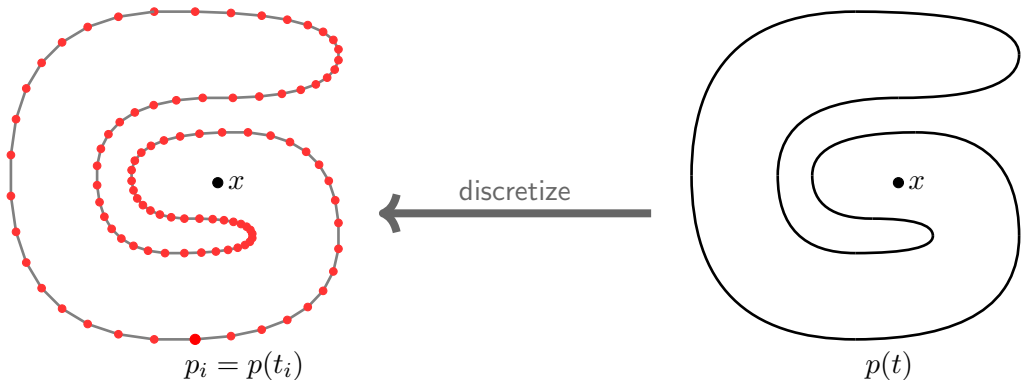
Curve: $\{p(t) : t \in [a, b]\}, p(a) = p(b)$

transfinite barycentric kernel $\lambda(x, t)$

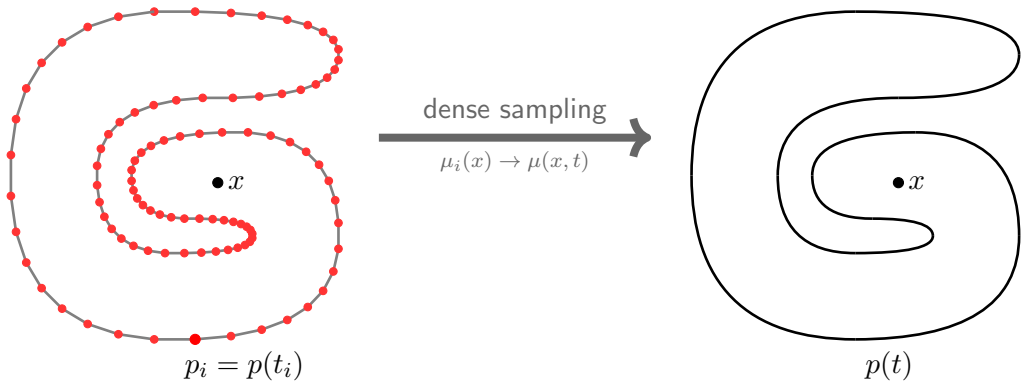
$$\int_a^b \mu(x, t)(p(t) - x) dt = 0$$

$$\lambda(x, t) = \mu(x, t) \Bigg/ \int_a^b \mu(x, s) ds$$

Discretize the continuous boundary



Discretize the continuous boundary



Related work

- ❖ Wachspress kernel [Warren et al., 2007]

$$\mu(x, t) = \frac{p'(t) \times p''(t)}{\left((p(t) - x) \times p'(t)\right)^2}$$

- ❖ Mean value kernel [Dyken and Floater, 2009]

$$\mu(x, t) = \frac{(p(t) - x) \times p'(t)}{\|p(t) - x\|^3}$$

- ❖ Laplace kernel [Kosinka and Bartoň, 2016]

$$\mu(x, t) = \frac{2\|p'(t)\|^2(p(t) - x) \times p'(t) - \|p(t) - x\|^2 p'(t) \times p''(t)}{\left((p(t) - x) \times p'(t)\right)^2}$$

Related work

- ❖ Wachspress kernel [Warren et al., 2007] *only for convex domains*

$$\mu(x, t) = \frac{p'(t) \times p''(t)}{\left((p(t) - x) \times p'(t)\right)^2}$$

- ❖ Mean value kernel [Dyken and Floater, 2009] *can be negative*

$$\mu(x, t) = \frac{(p(t) - x) \times p'(t)}{\|p(t) - x\|^3}$$

- ❖ Laplace kernel [Kosinka and Bartoň, 2016] *only for convex domains*

$$\mu(x, t) = \frac{2\|p'(t)\|^2(p(t) - x) \times p'(t) - \|p(t) - x\|^2 p'(t) \times p''(t)}{\left((p(t) - x) \times p'(t)\right)^2}$$

Related work

- ❖ Gordon–Wixom interpolation [Gordon and Wixom, 1974]

$$g_{1,-1}(x, \theta) = \left(\frac{f(y_1)}{d_1} + \frac{f(y_{-1})}{d_{-1}} \right) \Big/ \left(\frac{1}{d_1} + \frac{1}{d_{-1}} \right), \quad g(x) = \frac{1}{2\pi} \int_0^{2\pi} g_{1,-1}(x, \theta) d\theta$$

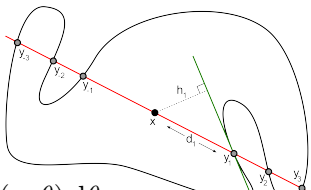
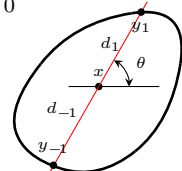
- ❖ Weighted Gordon–Wixom interpolation [Belyaev, 2006]

$$g(x) = \int_0^{2\pi} g_{1,-1}(x, \theta) \omega(x, \theta) d\theta \Big/ \int_0^{2\pi} \omega(x, \theta) d\theta$$

- ❖ Positive Gordon–Wixom kernel [Manson et al., 2011]

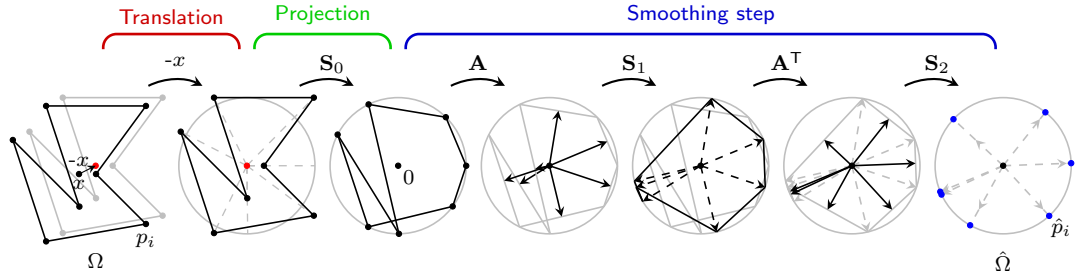
$$g_{i,j}(x, \theta) = \left(\frac{f(y_i)}{d_i} + \frac{f(y_{-j})}{d_{-j}} \right) \Big/ \left(\frac{1}{d_i} + \frac{1}{d_{-j}} \right)$$

$$g(x) = \int_0^{2\pi} \sum_{i=1}^m \sum_{j=-n}^{-1} g_{i,j}(x, \theta) \omega_{i,j}(x, \theta) d\theta \Big/ \int_0^{2\pi} \sum_{i=1}^m \sum_{j=-n}^{-1} \omega_{i,j}(x, \theta) d\theta$$



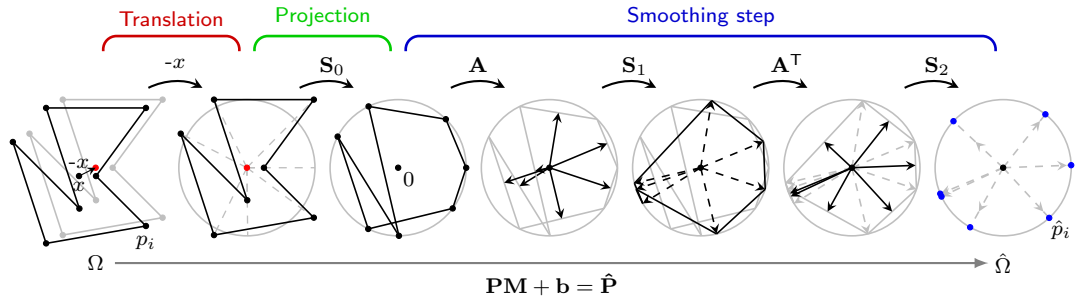
Discrete max-likelihood coordinates

[Chang et al., 2023]



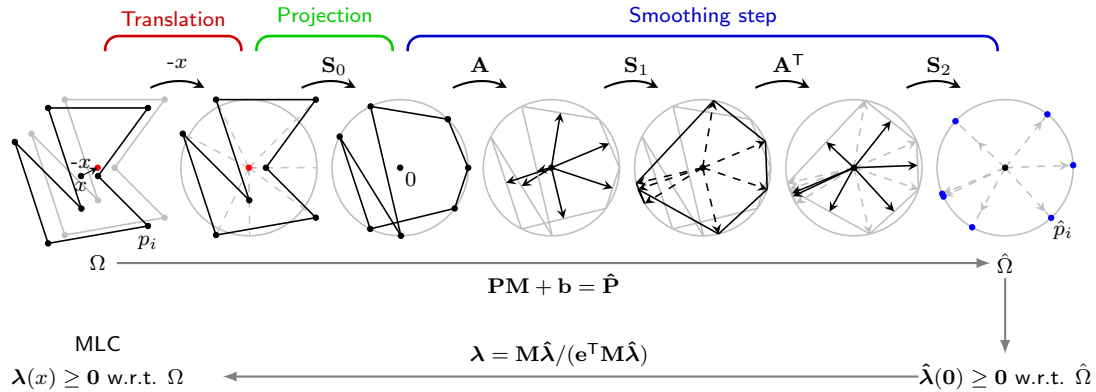
Discrete max-likelihood coordinates

[Chang et al., 2023]



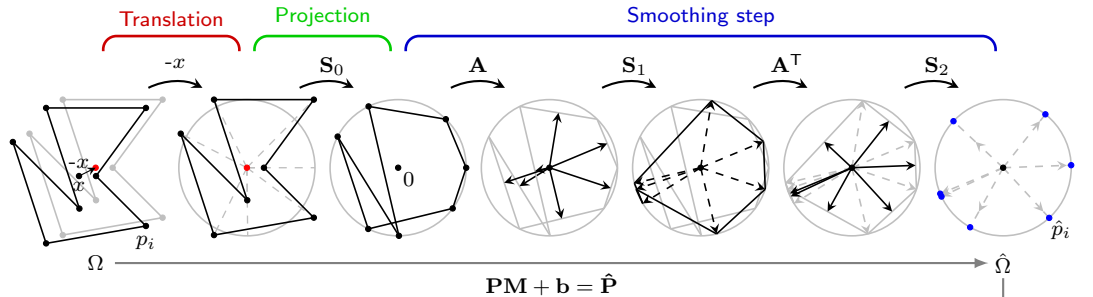
Discrete max-likelihood coordinates

[Chang et al., 2023]



Discrete max-likelihood coordinates

[Chang et al., 2023]



$$\text{MLC}$$

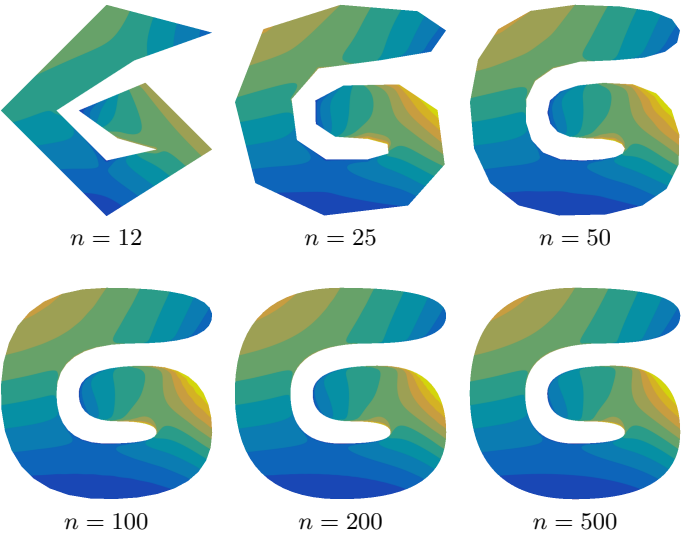
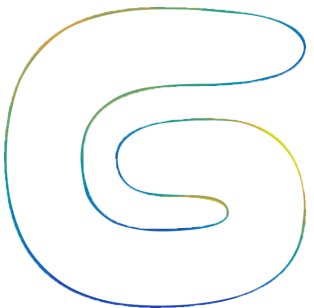
$$\lambda(x) \geq 0 \text{ w.r.t. } \Omega$$

$$\lambda = \mathbf{M}\hat{\lambda}/(\mathbf{e}^\top \mathbf{M}\hat{\lambda})$$

$$\hat{\lambda}(0) \geq 0 \text{ w.r.t. } \hat{\Omega}$$

$$\hat{\lambda} = \arg \max_{\hat{\lambda}} \sum_{i=1}^n \log \hat{\lambda}_i \quad \text{s.t.} \quad \sum_{i=1}^n \hat{\lambda}_i \hat{p}_i = 0, \quad \sum_{i=1}^n \hat{\lambda}_i = 1$$

Discrete maximum likelihood interpolation



Extension to continuous boundaries

- ❖ Translate and project the boundary onto the unit circle oriented at $\mathbf{0}$

$$\hat{p}(t) = \frac{p(t) - x}{r(x, t)}, \quad r(x, t) = \|p(t) - x\|$$

- ❖ Smooth the adjacent points (not needed)
- ❖ Compute $\hat{\lambda}(t)$ by maximizing the likelihood function

$$\ell[\hat{\lambda}] = \int_a^b \log \hat{\lambda}(t) dt \quad \text{s.t.} \quad \int_a^b \hat{\lambda}(t) \hat{p}(t) dt = \mathbf{0}, \quad \int_a^b \hat{\lambda}(t) dt = 1$$

- ❖ Compute the barycentric kernel $\lambda(x, t)$ over the original boundary

$$\lambda(x, t) = \frac{\hat{\lambda}(t)}{r(x, t)} \Bigg/ \int_a^b \frac{\hat{\lambda}(s)}{r(x, s)} ds$$

Extension to continuous boundaries

- ❖ Translate and project the boundary onto the unit circle oriented at 0

$$\hat{p}(t) = \frac{p(t) - x}{r(x, t)}, \quad r(x, t) = \|p(t) - x\|$$

- ❖ Smooth the adjacent points (not needed)

- ❖ Compute $\hat{\lambda}(t)$ by maximizing the likelihood function

Positive weight function

$$\ell[\hat{\lambda}] = \int_a^b \log \hat{\lambda}(t) \mathbf{w}(t) dt \quad \text{s.t.} \quad \int_a^b \hat{\lambda}(t) \hat{p}(t) \mathbf{w}(t) dt = \mathbf{0}, \quad \int_a^b \hat{\lambda}(t) \mathbf{w}(t) dt = 1$$

- ❖ Compute the barycentric kernel $\lambda(x, t)$ over the original boundary

$$\lambda(x, t) = \frac{\hat{\lambda}(t) \mathbf{w}(t)}{r(x, t)} \Bigg/ \int_a^b \frac{\hat{\lambda}(s) \mathbf{w}(s)}{r(x, s)} ds$$

Extension to continuous boundaries

☞ Problem.1: How to solve the optimization problem?

☞ Problem.2: How to choose the weight function?

❖ Compute $\hat{\lambda}(t)$ by maximizing the likelihood function

$$\ell[\hat{\lambda}] = \int_a^b \log \hat{\lambda}(t) \mathbf{w}(t) dt \quad \text{s.t.} \quad \int_a^b \hat{\lambda}(t) \hat{p}(t) \mathbf{w}(t) dt = \mathbf{0}, \quad \int_a^b \hat{\lambda}(t) \mathbf{w}(t) dt = 1$$

❖ Compute the barycentric kernel $\lambda(x, t)$ over the original boundary

$$\lambda(x, t) = \frac{\hat{\lambda}(t) \mathbf{w}(t)}{r(x, t)} \Bigg/ \int_a^b \frac{\hat{\lambda}(s) \mathbf{w}(s)}{r(x, s)} ds$$

Solving the optimization problem

With the *Lagrange multipliers method* and the *Euler-Lagrange equation*

$$\hat{\lambda}(t) = \frac{1}{\phi_0 + \phi^\top \hat{p}(t)}, \quad \phi_0 = \int_a^b w(t) dt$$

Solving the optimization problem

With the *Lagrange multipliers method* and the *Euler-Lagrange equation*

$$\hat{\lambda}(t) = \frac{1}{\phi_0 + \phi^\top \hat{p}(t)}, \quad \phi_0 = \int_a^b w(t) dt$$

The ϕ can be computed by minimizing the function

$$\phi = \arg \min_{\phi \in \Phi} F(\phi), \quad F(\phi) = - \int_a^b \log(\phi_0 + \phi^\top \hat{p}(t)) w(t) dt$$

Solving the optimization problem

With the *Lagrange multipliers method* and the *Euler-Lagrange equation*

$$\hat{\lambda}(t) = \frac{1}{\phi_0 + \phi^\top \hat{p}(t)}, \quad \phi_0 = \int_a^b w(t) dt$$

The ϕ can be computed by minimizing the function

$$\phi = \arg \min_{\phi \in \Phi} F(\phi), \quad F(\phi) = - \int_a^b \log(\phi_0 + \phi^\top \hat{p}(t)) w(t) dt$$

The domain of F is a **circle** with radius ϕ_0 centered at the origin

$$\Phi = \{\phi \in \mathbb{R}^2 \mid \|\phi\| \leq \phi_0\}$$

Solving the optimization problem

With the *Lagrange multipliers method* and the *Euler-Lagrange equation*

$$\hat{\lambda}(t) = \frac{1}{\phi_0 + \phi^\top \hat{p}(t)}, \quad \phi_0 = \int_a^b w(t) dt$$

The ϕ can be computed by minimizing the function

$$\phi = \arg \min_{\phi \in \Phi} F(\phi), \quad F(\phi) = - \int_a^b \log(\phi_0 + \phi^\top \hat{p}(t)) w(t) dt$$

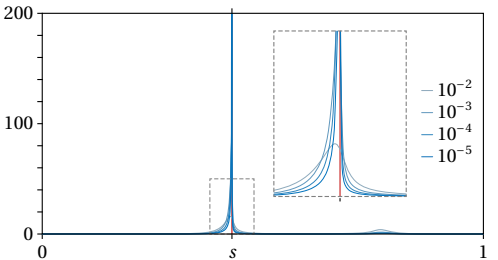
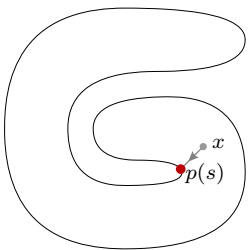
The domain of F is a **circle** with radius ϕ_0 centered at the origin

$$\Phi = \{\phi \in \mathbb{R}^2 \mid \|\phi\| \leq \phi_0\}$$

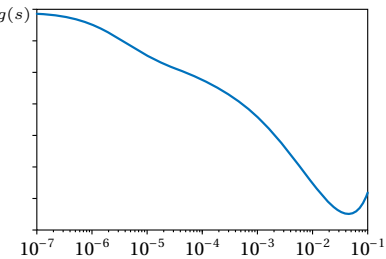
$F(\phi)$: strictly convex function Newton method

❖ Constant weight function

$$w_x(t) = 1$$



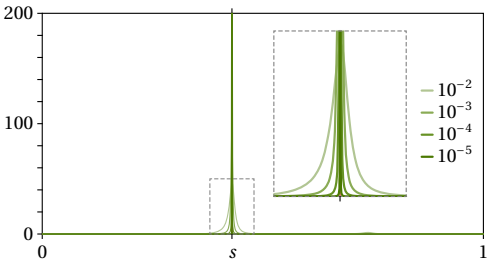
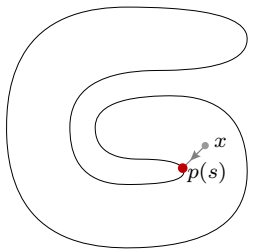
$\lambda(x, t)$ converges **slowly** to δ function



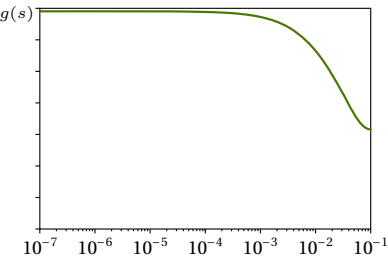
$g(x)$ converges **slowly** to $g(s)$

❖ Inverse distance weight function

$$w_x(t) = \frac{1}{r(x, t)}$$



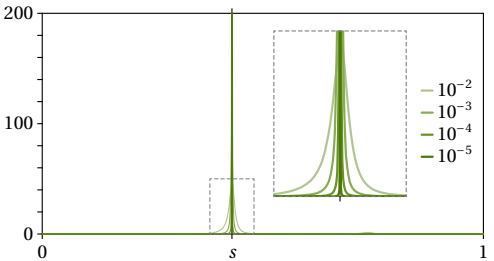
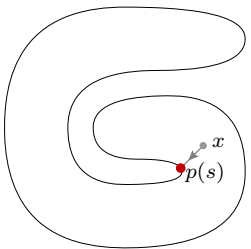
$\lambda(x, t)$ converges quickly to δ function



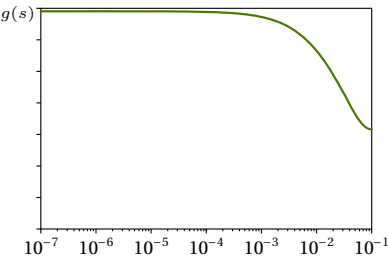
$g(x)$ converges quickly to $g(s)$

❖ Inverse distance weight function

$$w_x(t) = \frac{1}{r(x, t)}$$



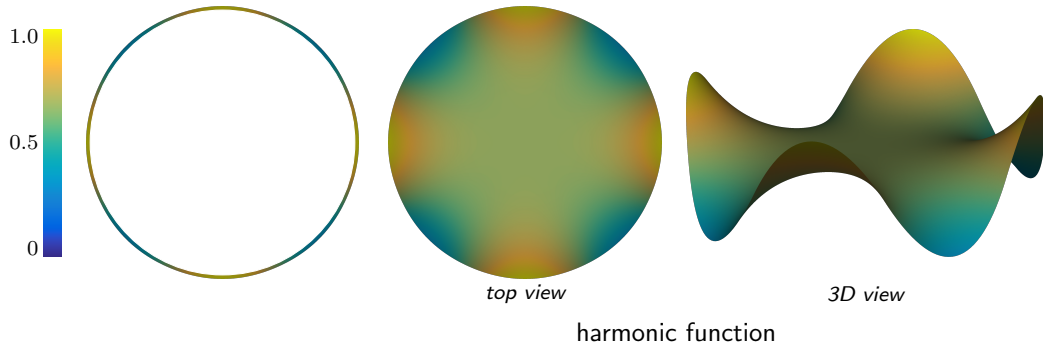
$\lambda(x, t)$ converges **quickly** to δ function



$g(x)$ converges **quickly** to $g(s)$

$\lambda(x, t)$ is a **pseudo-harmonic kernel**

❖ Inverse distance weight function

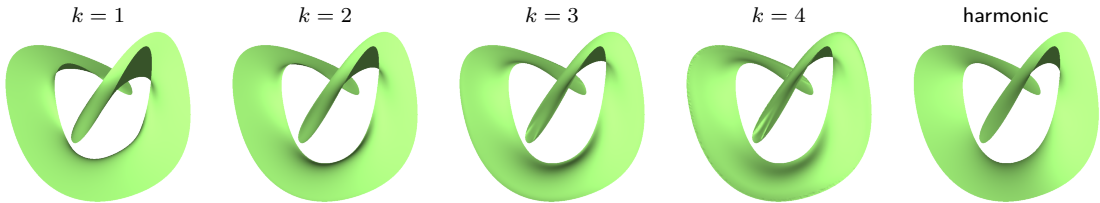


❖ ***k*-th power of inverse distance weight function**

$$w_x(t) = \frac{1}{r(x, t)^k}$$

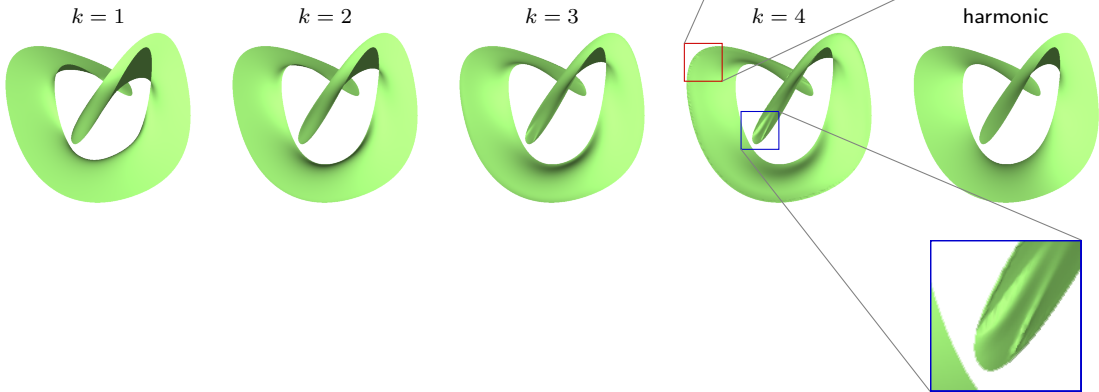
❖ *k*-th power of inverse distance weight function

$$w_x(t) = \frac{1}{r(x, t)^k}$$



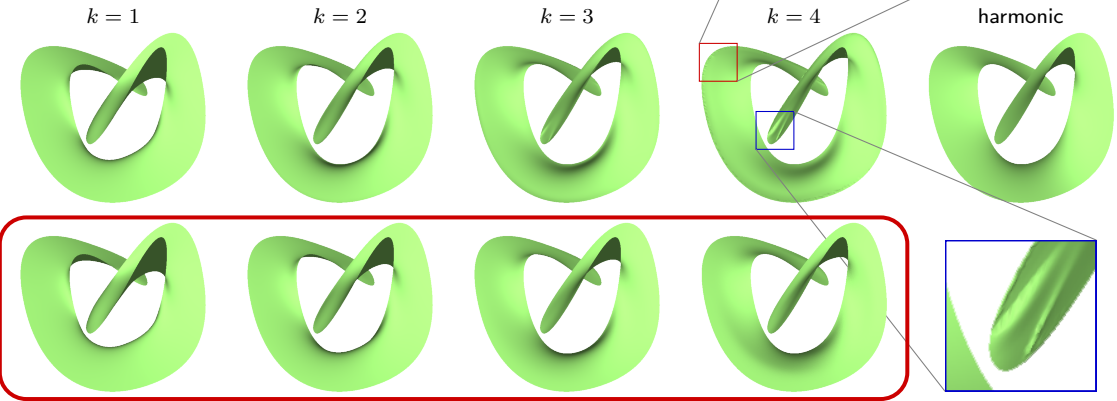
❖ k -th power of inverse distance weight function

$$w_x(t) = \frac{1}{r(x, t)^k}$$



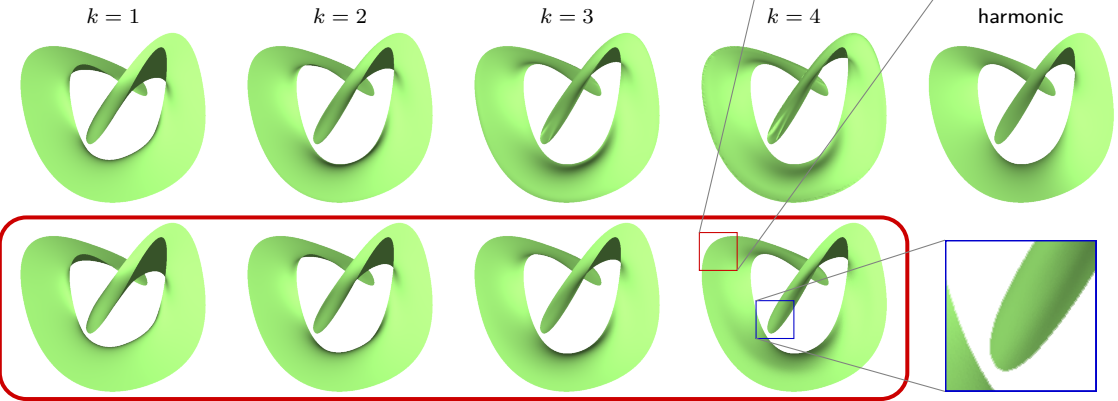
❖ Modified k -th power of inverse distance weight

$$w_x(t) = \frac{1}{r(x, t)^k} + \int_a^b \frac{1}{r(x, s)^k} ds$$



❖ Modified k -th power of inverse distance weight

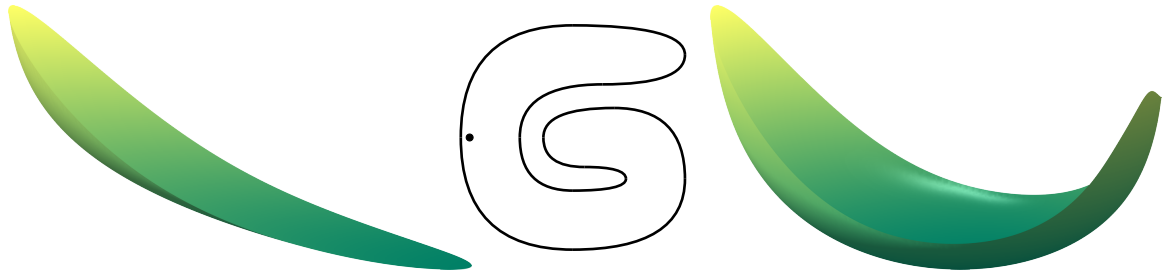
$$w_x(t) = \frac{1}{r(x, t)^k} + \int_a^b \frac{1}{r(x, s)^k} ds$$



Reason for improving stability

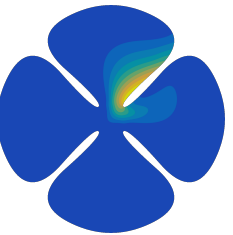
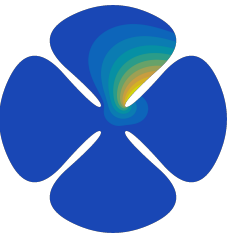
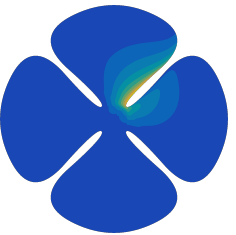
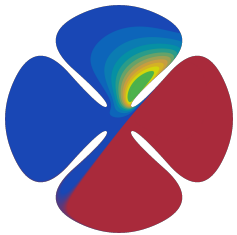
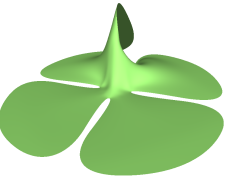
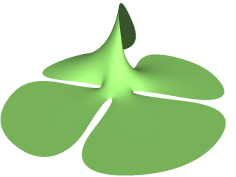
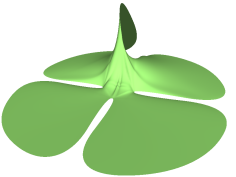
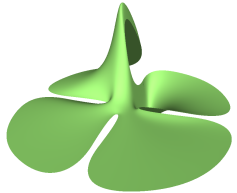
$$w_x(t) = \frac{1}{r(x,t)^4}$$

$$w_x(t) = \frac{1}{r(x,t)^4} + \int_a^b \frac{1}{r(x,s)^4} \mathrm{d}s$$



$$F(\phi) = - \int_a^b \log(\phi_0 + \phi^\top \hat{p}_x(t)) w_x(t) \mathrm{d}t$$

Experiments - Comparison of interpolation



mean value kernel

positive Gordon–Wixom

Poisson kernel

$$w_x(t) = \frac{1}{r^4} + \int_a^b \frac{1}{r^4} ds$$

Experiments - Interpolating polygonal boundary domain

generalized barycentric coordinates



mean value kernel



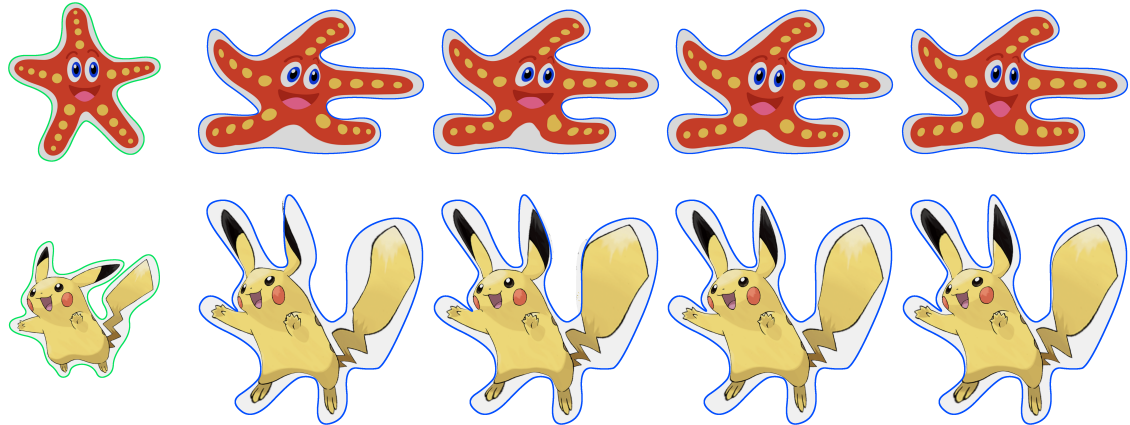
positive Gordon–Wixom



Poisson kernel

$$w_x(t) = \frac{1}{r^4} + \int_a^b \frac{1}{r^4} ds$$

Experiments - Comparison of image deformation



source

mean value kernel

positive Gordon–Wixom

Poisson kernel

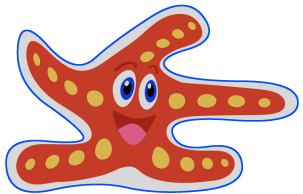
$$w_x(t) = \frac{1}{r^4} + \int_a^b \frac{1}{r^4} ds$$

Conclusion

- ❖ Extend maximum likelihood coordinates to arbitrary closed domains
 - ◆ Variational problem (*Lagrange multipliers method; Euler-Lagrange equation*)
- ❖ By introducing a weight function, we get different results
 - ◆ Constant weight function (*equivalent to the discrete maximum likelihood coordinates*)
(convergence slowly to the δ function at the boundary.)
 - ◆ Inverse distance weight (*pseudo-harmonic kernel*)
 - ◆ k -th power of inverse distance weight (*unstable optimization*)
 - ◆ Modified k -th power of inverse distance weight (*stable optimization*)
- ❖ Parameterization-dependent
 - ◆ The natural parameterization is good enough for most cases
 - ◆ More freedom for the users

Positive & Smooth

Thank you!



Running time

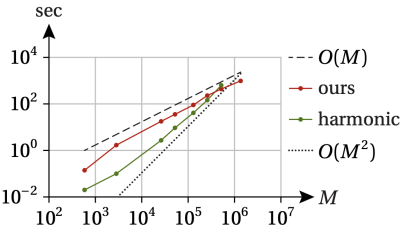
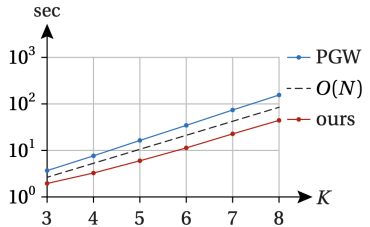


Figure 7: Running time in seconds for evaluating our interpolants and the PGW interpolant based on $N = 2^K 12$ boundary samples at 26000 domain points (left) and for computing the piecewise linear approximation of our interpolants and the harmonic interpolant over a domain triangulation with M vertices (right).

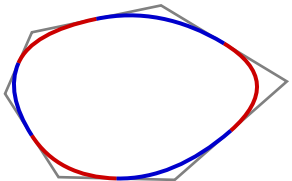
Experiments - Construct boundary and boundary data

Using quadratic B-splines for describing both the boundary and the boundary data

- ❖ Construct boundary

$$p(t) = \sum_{i=0}^{n+1} p_i B_i(t)$$

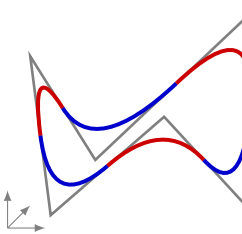
$$(p_0 := p_n, \ p_{n+1} := p_1)$$



- ❖ Specific boundary data

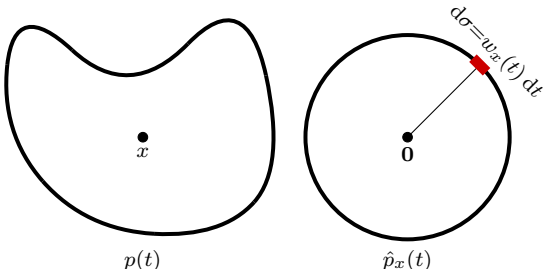
$$f(t) = \sum_{i=0}^{n+1} f_i B_i(t)$$

$$(f_0 := f_n, \ f_{n+1} := f_1)$$



❖ Arc length differential weight function

$$w_x(t) = \|\hat{p}_x'(t)\|$$



$$\arg \max \ell[b_x] = \oint_{\hat{p}_x} \log k_x \, d\sigma$$

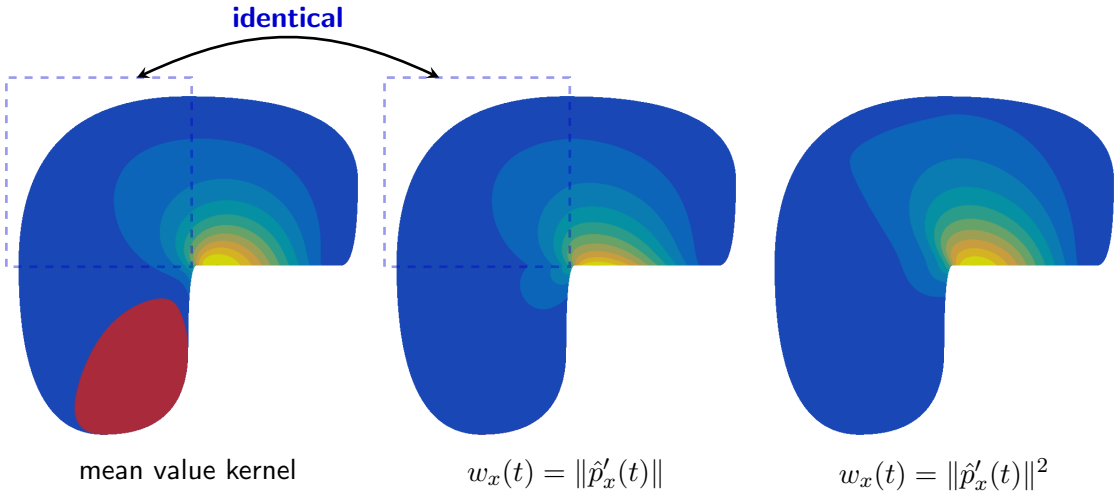
$$\text{s.t. } \oint_{\hat{p}_x} k_x \, d\sigma = 1,$$

$$\oint_{\hat{p}_x} k_x \cdot \sigma \, d\sigma = \mathbf{0}.$$

$$w_x(t) = \frac{|(p(t) - x) \times p'(t)|}{r(x,t)^2} = |\mu(x,t)| r(x,t)$$

$\mu(x,t)$ is **mean value kernel**

❖ Arc length differential weight function



How different parameterizations affect the results

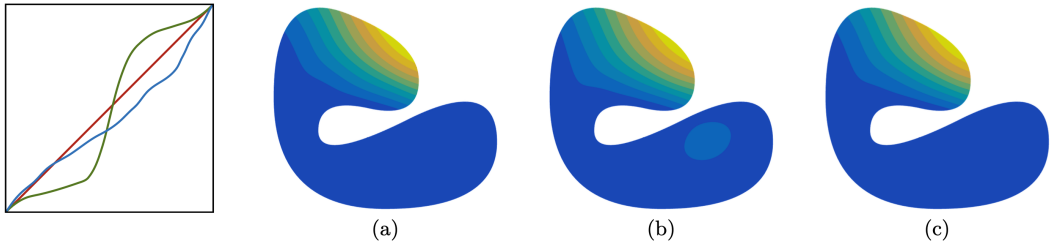


Figure 12: Transfinite basis function for our kernel with ω_x in (20) using the natural (red) parameterization of the boundary spline curve (a), after applying a monotonic (green) reparameterization (b), which creates a significant local maximum in the bottom right part of the domain, and after applying the arc-length (blue) reparameterization (c), which has little effect on the result in this example.



Belyaev, A. (2006).

On transfinite barycentric coordinates.

In *Proceedings of the Fourth Symposium on Geometry Processing*, SGP '06, pages 89–99, Aire-la-Ville. Eurographics Association.



Chang, Q., Deng, C., and Hormann, K. (2023).

Maximum likelihood coordinates.

Computer Graphics Forum, 42(5):Article e14908, 13 pages.



Dyken, C. and Floater, M. S. (2009).

Transfinite mean value interpolation.

Computer Aided Geometric Design, 26(1):117–134.



Gordon, W. J. and Wixom, J. A. (1974).

Pseudo-harmonic interpolation on convex domains.

SIAM Journal on Numerical Analysis, 11(5):909–933.



Kosinka, J. and Bartoň, M. (2016).

Convergence of barycentric coordinates to barycentric kernels.

Computer Aided Geometric Design, 43:200–210.





Manson, J., Li, K., and Schaefer, S. (2011).

Positive Gordon–Wixom coordinates.

Computer-Aided Design, 43(11):1422–1426.

— The PGW source code is available at

http://josiahmanson.com/research/gordon_wixom_coords/.



Warren, J., Schaefer, S., Hirani, A. N., and Desbrun, M. (2007).

Barycentric coordinates for convex sets.

Advances in Computational Mathematics, 27(3):319–338.

